North–south topographic slope asymmetry on Mars: Evidence for insolation-related erosion at high obliquity

M. A. Kreslavsky

Department of Geological Sciences, Brown University, Providence, Rhode Island, USA

Astronomical Institute, Kharkov National University, Kharkov, Ukraine

J. W. Head

Department of Geological Sciences, Brown University, Providence, Rhode Island, USA

Received 22 May 2003; accepted 14 July 2003; published 12 August 2003.

[1] A map of north–south subkilometer-scale slope asymmetry on Mars obtained from statistical analysis of along-track MOLA topographic profiles reveals well-defined zonal belts of north–south slope asymmetry at 40–50° latitude in both hemispheres. In these narrow anomalous belts the pole-facing slopes are systematically gentler than equator-facing slopes. This asymmetry is especially pronounced for the steepest (>20°) slopes, in which pole-facing slopes are three times less frequent than >20° slopes facing the equator. We interpret these belts to be related to insolation asymmetry. Specifically, we suggest that summertime melting of ground ice on pole-facing slopes occurred during periods of very high obliquity (~45°) in the past and favored downslope movement of material and reduction of steep pole-facing slopes. *INDEX TERMS:* 5416 Planetology: Solid Surface Planets: Glaciation; 5415 Planetology: Solid Surface Planets: Erosion and weathering; 5450 Planetology: Solid Surface Planets: Orbital and rotational dynamics; 6225 Planetology: Solar System Objects: Mars. **Citation:** Kreslavsky, M. A., and J. W. Head, North–south topographic slope asymmetry on Mars: Evidence for insolation-related erosion at high obliquity, *Geophys. Res. Lett.*, *30*(15), 1815, doi:10.1029/2003GL017795, 2003.

1. Introduction

[2] Anisotropy of local slopes reflects the nature of topography-shaping processes. For example, asymmetry of opposite slopes is typical for eolian features such as dunes. North–south slope asymmetry is also an important indicator of processes related to insolation and water mobility. For example, asymmetric troughs in the polar cap deposits of Mars have been interpreted to be due to insolation-related sublimation (producing steep equator-facing slopes) and deposition (producing gentle pole-facing slopes) [e.g., *Howard et al.*, 1982]. In this study we used the MOLA data set to map globally and analyze slope asymmetry on Mars.

2. Data Processing

[3] The Mars Orbiter Laser Altimeter (MOLA) onboard the Mars Global Surveyor (MGS) spacecraft produced a large homogeneous data set of precise elevation measurements along MGS tracks [e.g., *Smith et al.*, 2001] with uniform along-track spacing of 0.3 km. Except for narrow zones at very high latitudes, the gaps between the tracks are often wider than the along-track spacing.

[4] The direction of all MOLA tracks is close to meridianal except in high-latitude regions. The deflection from the meridian is about 5° in a wide equatorial zone. Poleward from 60° latitude, the deflection increases slowly, then more rapidly, and reaches 17° at 80° latitude. Thus, sampling of the Mars surface with MOLA is strongly anisotropic. Track-to-track systematic errors in a wide equatorial zone are greater than the noise of along-track measurements even after crossover analysis [*Neumann et al.*, 2001]. This means that kilometer-scale slopes derived from the gridded topographic map are affected by strongly anisotropic errors. The slopes along individual orbital tracks, however, are free of such errors, and the MOLA data can be effectively used to study the north–south asymmetry of the slopes at kilometer- and hectometer-scale baselines.

[5] The data processing technique we used was similar to that applied by *Kreslavsky and Head* [2000, 2002]. For each pair of consecutive MOLA shots, we calculated the differential slope; a positive sign was used for the south-facing slopes, and negative for north-facing slopes. The differential slope s was defined (Figure 1, left) through slope α at 0.3 km baseline (the shot-to-shot distance) and slope β at 0.9 km baseline as: $\tan s = \tan \alpha - \tan \beta$. The use of the differential slope s instead of the ordinary slope α was necessary to eliminate the influence of regional topography on slope statistics. The present definition of the differential slope is slightly different from that used by *Kreslavsky and Head* [2000] and permits the use of the shortest possible baseline length of 0.3 km.

[6] All calculated slopes were binned into 0.25° × 0.25° map cells; for each cell we calculated the median slope $q_{1/2}$ and the quartiles $q_{1/4}$ and $q_{3/4}$ of the slope-frequency distribution (Figure 1, right).

[7] The difference between the quartiles $r = q_{3/4} - q_{1/4}$ characterizes the width of the slope-frequency distribution, and serves as a measure of roughness [e.g., *Neumann and Forsyth*, 1995]. Figure 2 shows the roughness map in a simple cylindrical projection obtained in this way; brighter shades denote rougher surfaces. Major geomorphic features are clearly distinguishable in the map; the latitudinal trend of roughness (smoother terrains at high latitudes) is pronounced even more clearly than in *Kreslavsky and Head* [2000] (their Figure 12), because the baseline used here is

0094-8276/03/2003GL017795$05.00

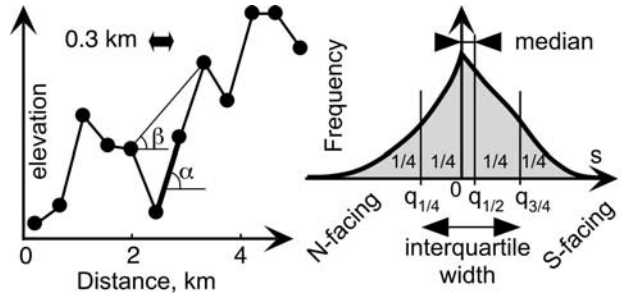

Figure 1. Left, a schematic MOLA profile showing local along-track slope α at 0.3 km baseline and slope β at 0.9 km baseline used to calculate the differential slope. Right, schematic differential-slope-frequency distribution showing the quartiles $q_{1/4}$ and $q_{3/4}$, and the median $q_{1/2}$.

twice shorter. See *Kreslavsky and Head* [2000] for further discussion of the roughness maps.

[8] The median signed slope $q_{1/2}$ can be used to quantify the deviation of the slope-frequency distribution shape from symmetric. The mean differential slope is almost exactly equal to zero. If the median slope is positive, this means that the number of south-facing profile segments is greater than the number of north-facing ones. Zero mean slope demands that the excess of the number of south-facing segments is compensated by their gentleness. Thus, the positive median slope means that the south-facing slopes are generally gentler than north-facing slopes (or, equivalently, north-facing slopes are steeper). Analogously, negative median slope means that north-facing slopes are gentler.

[9] To eliminate roughness and characterize solely the distribution shape we normalized the median by the quartile difference and calculate the asymmetry parameter $a = q_{1/2}/r$. The map of this parameter is shown in Figure 3; brighter shades denote positive a, that is that north-facing slopes are steeper, and darker shades denote that south-facing slopes are steeper.

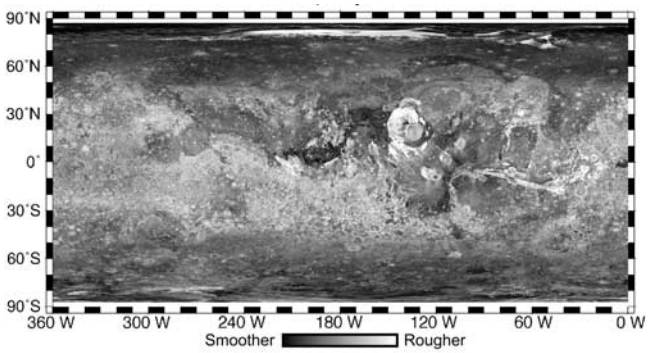

Figure 2. Map of roughness at 0.3 km baseline. Brighter shades denote rougher surface.

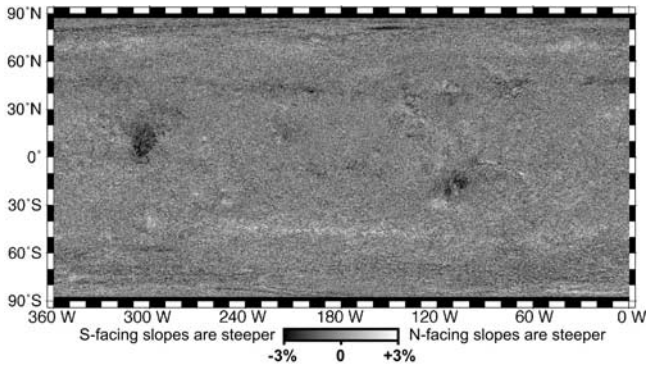

Figure 3. Map of the north–south slope asymmetry parameter a. Brighter shades denote that north-facing slopes are steeper; darker shades denote that south-facing slopes are steeper.

3. Regions of Slope Asymmetry

[10] The map of slope asymmetry (Figure 3) shows clearly that most of the surface does not have any north–south slope asymmetry. Several distinctive areas, however, clearly show slope asymmetry. We repeated our calculations for longer baselines (0.6 km and 1.2 km) and obtained a spatial asymmetry distribution very similar to that shown in Figure 3, but characteristic values of the asymmetry parameter $|a|$ were systematically lower than for a 0.3 km baseline. For even longer baselines, the calculated parameter a reflects mostly walls of steep topographic features, like major graben, channels, craters, etc.

3.1. Regional Anomalies

[11] The highest calculated absolute values of the asymmetry parameter $a \approx -5\%$ are in a compact area at $\sim$80°N 140–160°W, in the eastern part of Olympia Planitia (Figure 3). This is due to the interference of the MGS track orientation with the strongly asymmetric topography of dunes [e.g., *Tsoar et al.*, 1979]. The other sand seas at high north latitudes do not show anisotropy because they are strongly undersampled by MOLA and/or the dunes are formed predominantly by westerly winds.

[12] The next strongest asymmetry is observed in a few regions in the equatorial zone. The region in south–east Arabia Terra (10°N 305°W) just to the west of Syrtis Major, and Syria Planum (15°S 95°W) have an asymmetry parameter $a \approx -2.5\%$; south-facing slopes are steeper in these areas. An anomaly of the same sign is observed in north–east Daedalia Planum (20°S 105°W), and of the opposite sign in south–east Daedalia Planum (30°S 105–115°W). The latter two areas are also known to be anomalous in another statistical characteristics of along-track MOLA topography: in this region there is a strong prevalence of concave topographic profiles [*Kreslavsky and Head*, 2002]. There are several less pronounced local anomalies.

[13] Detailed study of the differential-slope-frequency distributions showed, that for typical highlands without asymmetry the positive and negative branches of the distribution are identical. For the anomalous areas in Arabia Terra, the difference between north- and south-facing slopes is small but noticable for gentle slopes, below $2r \approx 1°$. For the other local anomalous areas mentioned above the character of asymmetry is similar to that of the area in south–east Arabia: the gentle and moderately steep slopes contribute to the observed asymmetry.

[14] Some even weaker but still distinguishable deflection of the asymmetry parameter a from zero is associated

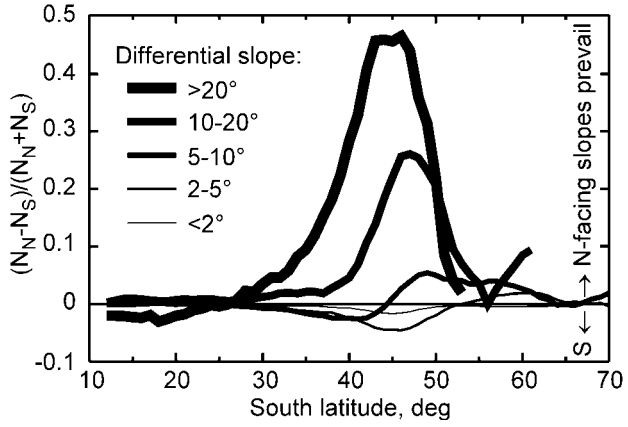

Figure 4. Asymmetry of differential slopes of different steepness in southern highlands within the 180–220°W sector calculated within 150-km wide latitudinal zones and plotted against latitude. The measure of asymmetry is $(N_N - N_S)/(N_N + N_S)$, where N_N and N_S are numbers of steep N- (equator-) and S- (pole-) facing segments in all MOLA profiles. Different curves correspond to different ranges of differential slopes, as shown. For gentle slopes (thin curves), S-facing slopes prevail around 45°S, providing the positive median slope, as mapped in Figure 3. For steep slopes (bold curves) a strong prevalence of N-facing slopes is observed at midlatitudes.

with extended regional slopes of major volcanic constructs on Mars: their northern slopes show some prevalence of positive values of a, and their southern slopes show negative values. This effect is best expressed in Alba Patera and the Elysium rise. It is clear that these long smooth regional slopes do not bias the differential slope values. Thus, the downslope-facing small-scale slopes are steeper here.

3.2. Latitudinal Anomalous Belts

[15] One of the most prominent features of the map is a pair of narrow latitudinal anomalous belts near 45° in both hemispheres. The signs of the median slope in both hemispheres are opposite indicating that pole-facing slopes are gentler in these zones. The intensity of asymmetry varies with longitude within these belts. The characteristic value of the asymmetry parameter a in prominent parts of the belts is $|a| \approx 0.8\%$. Both belts show a small deflection from ~45° parallel to the south in the western hemisphere and to the north in the eastern one. The bands are well approximated by minor circles with the centers shifted ~5° from the poles toward 60–90°W in the northern hemisphere and to the opposite direction in the southern hemisphere.

[16] The character of asymmetry in these belts differs from that of the regional anomalies. The low-slope (<1–2°) portion of the frequency distribution of the differential slopes for the anomalous belts is symmetrical, while asymmetry is observed for steeper slopes. To study the role of steep slopes in the anomalous belts, we calculated the total number of MOLA profile segments for several steepness bins in narrow latitudinal zones. We limited these calculations to a geologically homogeneous region within southern heavily cratered highlands. We plotted a measure of misbalance of north- and south-facing profile segments against the latitude (Figure 4). It is seen that the small prevalence of pole-facing profile segments in the gentle slope bins is compensated by the very strong shortage of pole-facing segments in the steep slope bins. Among profile segments steeper than 20° around 45°S latitude, the number of pole-facing segments is almost a factor of three smaller than the number of equator-facing ones. Thus, the weak asymmetry seen in the map (Figure 3) is accompanied by a much stronger asymmetry that occurs for the steepest slopes.

[17] The anomalous belts are within a wider transitional zone (30–60°) between smoothed circumpolar regions and an unsmoothed equatorial zone (see Figure 2; also *Kreslavsky and Head* [2000, 2002]). The contrast between the rough equatorial and smooth high-latitude zones is especially pronounced for the steepest slopes (>~20°), which practically disappear above 50° latitude (Figure 5). When we move from the equator to the poles, the abundance of steep slopes drops down earlier for the pole-facing slopes and later for the equator-facing slopes (Figure 5). This produces the observed strong asymmetry in steep slope abundance (Figure 4).

4. Discussion

[18] Is there morphological evidence for the causes of the slope asymmetry presented here? High-resolution images (e.g., MGS MOC-NA camera images [*Malin and Edgett*, 2001]) illustrating individual examples of geological processes that might produce the statistical slope asymmetries are at substantially different scales. This precludes the direct correlation of specific slope asymmetry values at ~30 km resolution (Figure 3) with individual geological features in specific MOC images, although regional characterizations and correlations can be made.

4.1. Regional Anomalies

[19] High-resolution MOC images show that Arabia Terra and the anomalous areas in eastern Daedalia Planum and Syria Planum are covered with dust or sand deposits [*Malin and Edgett*, 2001]. Recent modeling of global atmospheric circulation at different obliquity [*Haberle et*

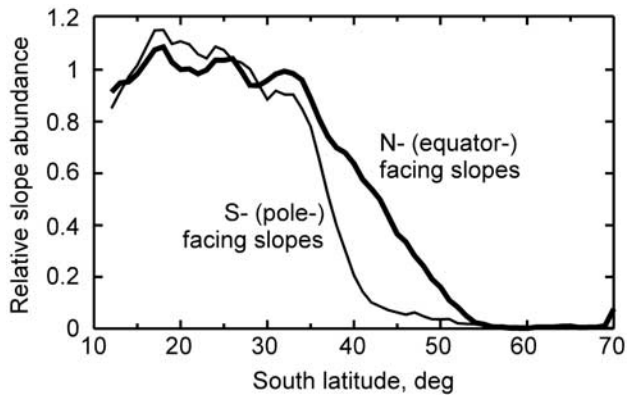

Figure 5. Abundance of steep N- and S- facing slopes relative to that of typical equatorial highlands plotted against latitude for Terra Cimmeria (180–220°W). The quantity actually plotted is the proportion of MOLA profile segments steeper than 20° at given latitude normalized by the same proportion for the 10°S–20°S zone. Bold and thin curves represent north- and south-facing slopes, respectively.

al., 2003] showed that Arabia Terra and the Tharsis rise (including Daedalia and Syria) are probable regions of dust deposition for all epochs in Martian history. Asymmetry of gentle slopes in this area could be caused by prevailing winds, a factor important in the formation of hectometer-scale topography. For the slopes of the major volcanic constructs, the regional slopes are an obvious natural cause of small-scale slope asymmetry. The observed asymmetry is, at least partly, due to downslope-facing lava flow fronts. Downslope mass movement and regional-topography-controlled winds can also contribute to the observed asymmetry. Detailed study of the regional anomalies will be published elsewhere.

4.2. Latitudinal Anomalous Belts

[20] The approximate symmetry relative to the equator strongly suggests that the role of insolation was important in the formation of the anomalous belts. The midlatitude zones (30–60°) that include the anomalous belts possess a number of peculiarities, and contain a number of different morphological features of zonal occurrence [e.g., *Mustard et al.*, 2001], including recent gullies [e.g., *Malin and Edgett*, 2001], which preferentially occur on pole-facing slopes. *Costard et al.* [2002] have interpreted these gullies to be due to melting of ground ice at higher obliquity. Their calculations showed that starting at ~35° obliquity, the summertime day-average surface temperature reaches 0°C at high (>~60°) latitudes; for higher obliquity the zero summer isotherm shifts toward the equator. The day-average temperature can exceed the ice melting point down to ~40° latitude at 45° obliquity, but only on steep pole-facing slopes.

[21] We suggest that transient melting of ground ice in summer during periods of high obliquity promotes downslope movement of material and lowers steep slopes. Over geological timescales, this process removed almost all steep slopes above 50° latitude. At 40–50° latitude, the summertime melting and related movement can occur only on pole-facing slopes, making these slopes less steep. The equator-facing slopes in this zone remain intact. This produces the observed strong asymmetry of the steepest slopes.

[22] Additional processes that could contribute to the observed steep slope asymmetry in the anomalous belts include creep (without melting) of thin sheets of ice-rich material on steep slopes [e.g., *Milliken et al.*, 2002]. During periods of moderately high obliquity, when atmospheric water is abundant, but pole-facing slopes are still colder in the summer, preferential H_2O frost and ice accumulation could occur on pole-facing slopes. This would favor glacial and periglacial modification of these slopes. The latter effect, however, cannot be solely responsible for the observed asymmetry, because it would not have so narrow a latitudinal occurrence.

[23] The deflection of the belts from 45° latitude could be related to effects of persistent atmospheric circulation or albedo patterns during the high obliquity epochs. Alternatively, taking into account the conclusion by *Bills and James* [1999] that the position of Mars rotation axis relative to the surface is secularly unstable, one can hypothesize that the current pole position is shifted ~5° from a formerly stable or long-term-average position. The direction of this shift is neither similar nor opposite to the shift of the geometric centers of the polar layered deposits [*Fishbaugh and Head*, 2001].

[24] In summary, narrow anomalous belts of slope asymmetry centered at 45° latitude in both hemispheres are plausibly interpreted to be due to insolation asymmetry at high obliquity (~45°) that favored downslope movement of material and reduce steep pole-facing slopes.

[25] **Acknowledgments.** Discussions with F. Costard were extremely helpful. The work was partly supported by NASA grant NAG5-12286.

References

Bills, B. G., and T. S. James, Moments of inertia and rotational stability of Mars: Lithospheric support of subhydrostatic rotational flattening, *J. Geophys. Res.*, *104*, 9081–9096, 1999.

Costard, F., F. Forget, N. Mangold, and L.-P. Peulvast, Formation of recent Martian debris flows by melting of near-surface ground ice at high obliquity, *Science*, *295*, 110–113, 2002.

Fishbaugh, K. E., and J. W. Head, Comparison of the North and South Polar Caps of Mars: New Observations from MOLA Data and Discussion of Some Outstanding Questions, *Icarus*, *154*, 145–161, 2001.

Haberle, R. M., J. R. Murphy, and J. Schaeffer, Orbital change experiments with a Mars general circulation model, *Icarus*, *161*, 66–89, 2003.

Howard, A. D., J. A. Cutts, and K. R. Balsius, Stratigraphic relationships within Martian polar cap deposits, *Icarus*, *50*, 161–215, 1982.

Kreslavsky, M. A., and J. W. Head, Kilometer-scale roughness of Mars' surface: Results from MOLA data analysis, *J. Geophys. Res.*, *105*, 26,695–26,712, 2000.

Kreslavsky, M. A., and J. W. Head, Mars: Nature and evolution of young latitude-dependent water-ice-rich mantle, *Geophys. Res.*, 29, 10.1029/2002GL015392, 2002.

Malin, M. C., and K. S. Edgett, Mars Global Surveyor Mars Orbiter Camera: Interplanetary cruise through primary mission, *J. Geophys. Res.*, *106*, 23,429–23,570, 2001.

Milliken, R. E., J. F. Mustard, and D. L. Goldsby, Examination of viscous flow features on the surface of Mars (abstract), *Lunar and Planetary Sci. XXXIII*, 1870, 2002.

Mustard, J. F., C. D. Cooper, and M. K. Rifkin, Evidence for recent climate change on Mars from the identification of youthful near-surface ground ice, *Nature*, *412*, 411–414, 2001.

Neumann, G. A., and D. W. Forsyth, High resolution statistical estimations of seafloor morphology: Oblique and ortogonal fabric on the mid-Atlantic ridge, *Marine Geophys. Res.*, *17*, 221–250, 1995.

Neumann, G. A., D. D. Rowlands, F. G. Lemoine, D. E. Smith, and M. T. Zuber, Crossover analysis of Mars Orbiter Laser Altimeter data, *J. Geophys. Res.*, *106*, 23,753–23,768, 2001.

Smith, D. E., Mars Orbiter Laser Altimeter: Experiment summary after the first year of global mapping of Mars, *J. Geophys. Res.*, *106*, 23,689–23,722, 2001.

Tsoar, H., R. Greeley, and A. R. Peterfreund, Mars: The north polar sand sea and related wind patterns, *J. Geophys. Res.*, *84*, 8167–8180, 1979.

J. W. Head and M. A. Krelavsky, Department of Geophysical Sciences, Brown University, Providence, Rhode Island, USA. (misha@mare.geo.brown.edu)